Contents

1   Overview

This document is meant to log my progress in the investigation of mechanical modes in crystals of hard regular polygon particles. The system consists of $N = n^2 \times n_{\text{unit}}$ particles, where n is some integer and n_{unit} is the number of particles in the unit cell. The system is initialized in its densest known packing and then the crystal vectors are enlarged by constant factors to achieve a prescribed packing fraction. The motion of particles is decomposed into $n \times n$ distinct Fourier modes. There are $3n_{\text{unit}}$ relevant fields to investigate. The first $2n_{\text{unit}}$ are phonon fields signified by $\tilde{\mathbf{u}} = (\tilde{u}_x, \tilde{u}_y)$ (if the number of particles per unit cell is greater than 1, then these fields are further indexed *i.e.* $\tilde{\mathbf{u}}^{\alpha,\beta,\gamma\cdots}$. The remaining n_{unit} fields are libron fields, signified by $\tilde{\theta}^{\alpha,\beta,\gamma\cdots}$. In the case of hexagons, $n_{\text{unit}} = 1$, and in the case of many other polygons including pentagons studied here, $n_{\text{unit}} = 2$.

The various control parameters in a simulation are n the number of unit cells along one side of the box, ϕ the packing fraction, s the number of simulation steps, and the polygon shape. The densest packing, and thus the crystal lattice vectors, are determined by the polygon. The real space lattice vectors given by $\mathbf{a}_1, \mathbf{a}_2$ are usually meant to be in the densest packing, $\phi_{\max}$. When the system is relaxed to a smaller packing fraction, the lattice vectors are presumed to be $\mathbf{a}_i(\phi) = \mathbf{a}_i \sqrt{\phi_{\max}/\phi}$. The reciprocal lattice vectors $\mathbf{G}_i$ are constructed from these real space lattice vectors, and the unit cell of the reciprocal lattice forms the Brillouin zone within which $\mathbf{k}$ vectors are sampled. The relevant $\mathbf{k}$ vectors to sample are $n_1\mathbf{G}_1/n + n_2\mathbf{G}_2/n$, where n_i are integers. This way, the same number of Fourier modes are sampled as there are degrees of freedom in the real space system.

The Fourier modes are analyzed by considering their correlation functions. In Monte Carlo, dynamical information is not available, so collective degrees of freedom need to be analyzed from

correlation functions by way of a kind of generalized law of equipartition. We assume that this hard particle system which is controlled exclusively by entropic interactions can be approximated by a harmonic Hamiltonian:

$$\mathcal{H} = \frac{1}{2m}p_i \delta_{ij} p_j + \frac{1}{2I}L_i \delta_{ij} L_j + \frac{1}{2}x_i K_{ij} x_j. \tag{1}$$

The first term is the translational kinetic energy and the second term is the rotational kinetic energy. The last term is a harmonic coupling by a $3N \times 3N$ matrix, and x_i represent both the particle positions and particle orientations. In thermal equilibrium, it is provable that

$$\langle x_i x_j \rangle = k_B T K_{ij}^{-1}. \tag{2}$$

The matrix K_{ij} is partially diagonalized by the Fourier transform with respect to the lattice vectors $\mathbf{a}_{1,2}(\phi)$, so we find that

$$\langle \tilde{x}_{\mu,\mathbf{k}}^* \tilde{x}_{\nu,\mathbf{k}} \rangle = C_{\mu\nu,\mathbf{k}} = k_B T K_{\mu\nu,\mathbf{k}}^{-1}. \tag{3}$$

This decomposes the large $3N \times 3N$ matrix K_{ij} into a block diagonal $n^2 \times n^2$ matrix whose diagonal elements are $3n_{\text{unit}} \times 3n_{\text{unit}}$ matrices $K_{\mu\nu}$. The modes $\tilde{x}_\mu$ can represent either $\tilde{\mathbf{u}}_x^{\alpha,\beta\cdots}$, $\tilde{\mathbf{u}}_y^{\alpha,\beta\cdots}$ or $\tilde{\theta}^{\alpha,\beta\cdots}$. The ultimate output of the analysis are the $K_{\mu\nu,\mathbf{k}}$, which are obtained by computing every correlation function of all modes of the same wave vector and inverting the resulting matrix $C_{\mu\nu,\mathbf{k}}$. The elements of $\mathbf{K_k}$ are the squares of the phonon and libron dispersion relations, *i.e.* they furnish $\omega^2(\mathbf{k})$ for all $\mathbf{k}$ sampled in the Brillouin zone and for all collective modes $\tilde{\mathbf{u}}^{\alpha,\beta\cdots}$ and $\tilde{\theta}^{\alpha,\beta\cdots}$.

The matrices $\mathbf{K_k}$ depend on the packing fraction ϕ, the number of particles N, and the number of Monte Carlo sweeps taken s. If s is too small, then there is not a sufficient number of statistically independent Monte Carlo frames to compute the elements of the correlation matrix $\mathbf{C}$. The effect of s will be explored in Section 3.

In principle, the matrix $\mathbf{C}$ should be independent of N (or equivalently n), but having larger N helps resolve $\mathbf{C}$ as a function of $\mathbf{k}$, the wavevector, as the Brillouin zone is more densely populated. The effect of N will be explored in Section 4.

The matrix $\mathbf{C}$ is most markedly affected by changes in the packing fraction. Because polygon crystals melt into various phases (hexatic, rotator, or plain fluid), particular elements of $\mathbf{C}$ should simply vanish across these transitions, which I will show leads to flat dispersion relations. That is, particular elements of $\mathbf{K_k}$ become independent of $\mathbf{k}$. The effect of packing fraction will be shown in Section 5.

One of the difficulties in discerning meaningful interpretations of $\mathbf{K_k}$ is obviously the high dimensionality of the matrix. It is necessarily symmetric, so it has $3n_{\text{unit}}(3n_{\text{unit}} + 1)/2$ independent components, each of which is a function of the two-dimensional $\mathbf{k}$. Even for the one-particle unit cell of the hexagon crystal, there are 6 independent elements of $\mathbf{K_k}$ that need to be explored. Luckily, at quadratic order, the phonon mode is uncoupled from the libron mode, so this reduces the 6 components to 4 components (this uncoupling will also be demonstrated explicitly in Section 6).

To alleviate the difficulty in plotting a large-dimensional object as a function of a two-dimensional object, I resorted to taking cross sections in the Brillouin zone and plotting each of the $3n_{\text{unit}}(3n_{\text{unit}}+1)/2$ elements in the same figure. A sample plot is shown in Figure 1. These should be interpreted as giving the square frequencies of collective modes.
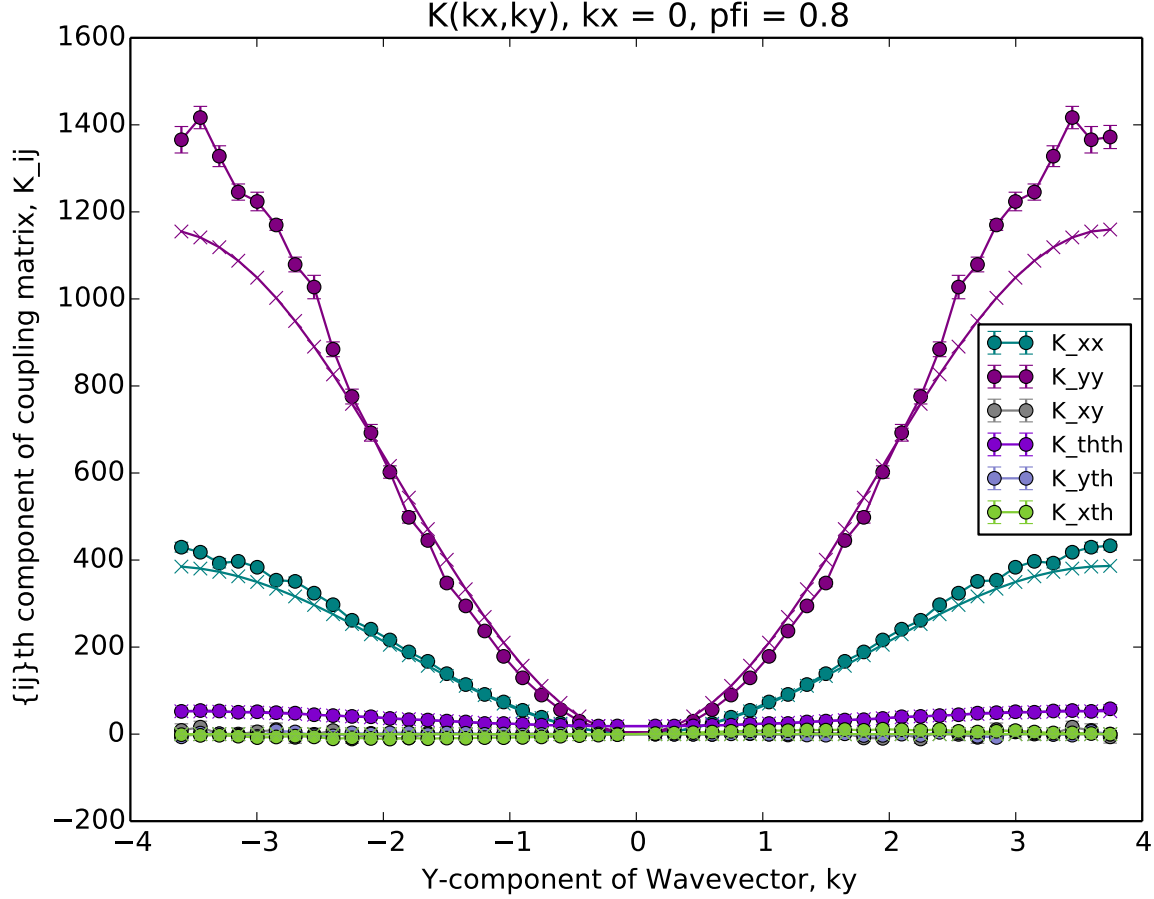

Figure 1: Sample figure for $\phi = 0.8$ (I used "pfi" for "packing fraction" and don't remember why I had the extra i). The curves marked with closed circles and error bars are from simulation data, and curves of the same color marked with x's are best-fit theoretical curves. The object K_{yy} is the dispersion curve for a longitudinal phonon traveling in the y direction (because here, the component $k_x = 0$), and K_{xx} is the dispersion for a transverse phonon. Along this particular axis in the Brillouin zone, the off-diagonal component K_{xy} is 0, but is displayed anyway. $K_{\theta\theta}$ is the dispersion for the libron, and because it is so much smaller than the phonon dispersion, we see that the libron is a more relaxed mode than the phonon. The off-diagonal elements $K_{x\theta}$ and $K_{y\theta}$ should also be 0 for all points in the Brillouin zone, but are also shown anyway. More plots will feature the θ elements zoomed in.

2 Theoretical model

The dispersion curves produced by the Fourier analysis described in Section 1 are fitted by a harmonic lattice model. A fundamental assumption of all the models is that the free energy of the system can be broken down into a sum of pairwise potentials between polygons that are close together. The simplest model assumes that this effective interaction energy is so close range that only nearest neighbors of the lattice feel each other. Furthermore, the two-body interaction potential is assumed to be at least twice-differentiable, so a harmonic approximation can be made. With the quadratic assumption, the dispersion curves can be calculated exactly as a function of only a couple parameters which correspond to second derivatives of the two-body potential. Lattices with high symmetry like the triangular lattice of hard hexagons have only 3 free parameters (1 for the phonons and 2 for the librons). In general, the theoretical matrix $\mathbf{K_k}$ is of the form

$$\mathbf{K_k} = \begin{pmatrix} K_{xx} & K_{xy} & K_{x\theta} \\ K_{xy} & K_{yy} & K_{y\theta} \\ K_{x\theta} & K_{y\theta} & K_{\theta\theta} \end{pmatrix} = \begin{pmatrix} 4\gamma_{xx} & 4\gamma_{xy} & 0 \\ 4\gamma_{xy} & 4\gamma_{yy} & 0 \\ 0 & 0 & 4\mu + 4\gamma \end{pmatrix}. \tag{4}$$

$$\gamma_{ij} = \frac{1}{2}\sum_{\mathbf{c}} A_{\mathbf{c}}\hat{c}_i\hat{c}_j \sin^2\left(\frac{\mathbf{k}\cdot\mathbf{c}}{2}\right), \quad \gamma = \frac{1}{2}\sum_{\mathbf{c}} E_{\mathbf{c}} \sin^2\left(\frac{\mathbf{k}\cdot\mathbf{c}}{2}\right), \quad \mu = \frac{1}{2}\sum_{\mathbf{c}} D_{\mathbf{c}} \cos^2\left(\frac{\mathbf{k}\cdot\mathbf{c}}{2}\right). \tag{5}$$

The off-diagonal elements used to contain parameters like $B, C,$ and F, but those ended up going to zero by symmetries, so I found myself in a similar boat to Maxwell, who had so many vector fields to deal with while formalizing electromagnetic theory that he just labeled them alphabetically. The constants $A_{\mathbf{c}}$, $E_{\mathbf{c}}$ and $D_{\mathbf{c}}$ depend on the vector $\mathbf{c}$ which separates two particles. In the hexagon lattice, all the nearest neighbors are the same by six-fold symmetry, so all of these parameters are independent of $\mathbf{c}$. In the pentagon lattice, the crystal only has two-fold symmetry, which brings us from 18 independent parameters to 9.

If we include next nearest neighbor interactions, then this introduces another set of constants that correspond to a second derivative of the effective interatomic pair potential, this time at a further distance. For both hexagons and pentagons, this would double the number of phenomenological constants to fit to. However, all of these constants appear as exterior multiplicative factors: the functional form of the dispersion curves are entirely predicted.

A key technical point is that for all the phonon dispersion curves, $\mathbf{k} = 0$ is a totally unaccessible mode, and is not shown in any plots. This is because the $\mathbf{k} = 0$ mode is a uniform translation. However, since the crystal can move any amount in the periodic simulation box, this mode is completely free. Because any particle motion in MC is a random event, the correlation function associated with the average position of the entire crystal will be arbitrarily small, so when it is inverted to give the phonon dispersion, the associated frequency is arbitrarily *large*. This divergence is totally artificial and a result of the simulation method, which does not preserve momentum conservation.

Here is a table of the simulations that have been completed. The rows vary in N and s, and the

columns vary in ϕ.

N s ϕ	0.850	0.800	0.750	0.710	0.700	0.690	0.680
$26^2,\, 3 \times 10^6$	$\checkmark$	$\checkmark$	$\checkmark$	$\checkmark$	$\checkmark$	$\checkmark$	$\times$
$50^2,\, 3 \times 10^6$	$\times$	$\times$	$\times$	$\times$	$\times$	$\times$	$\times$
$100^2,\, 3 \times 10^6$	$\times$	$\times$	$\times$	$\times$	$\times$	$\times$	$\times$
$26^2,\, 1 \times 10^7$	$\checkmark$	$\checkmark$	$\checkmark$	$\checkmark$	$\checkmark$	$\checkmark$	$\checkmark$
$50^2,\, 1 \times 10^7$	$\checkmark$	$\checkmark$	$\checkmark$	$\checkmark$	$\checkmark$	$\checkmark$	$\checkmark$
$100^2,\, 1 \times 10^7$	$\checkmark$	$\checkmark$	$\checkmark$	$\checkmark$	$\checkmark$	$\checkmark$	$\checkmark$
$26^2,\, 3 \times 10^7$	$\checkmark$	$\times$	$\times$	$\checkmark$	$\checkmark$	$\times$	$\times$
$50^2,\, 3 \times 10^7$	$\times$	$\times$	$\times$	$\times$	$\times$	$\times$	$\times$
$100^2,\, 3 \times 10^7$	$\times$	$\times$	$\times$	$\times$	$\times$	$\times$	$\times$

3   Small sampling effects

In a given simulation, s is the number of Monte Carlo sweeps, and snapshots are taken at a period such that there are $10^3/2$ presumably statistically independent frames to make correlation functions from. 10^3 frames are taken but only the latter half of them are used to compute correlation functions from, as to ensure the the simulations have equilibrated. Therefore, every sampled frame is separated a period of $T = s \times 10^{-3}$ sweeps. If this period is too small, frames won't be sufficiently independent from each other and spurious correlations will be introduced. However, if T is needlessly long, simulation time is wasted. Below are some plots of the dispersion curves at various packing fractions for hexagons. Keep in mind that at around $\phi = 0.700$–0.710 the crystal melts into a hexatic phase. It's not unreasonable that critical slowing down may occur near this transition point, and so shorter simulations may vary from longer simulations significantly.
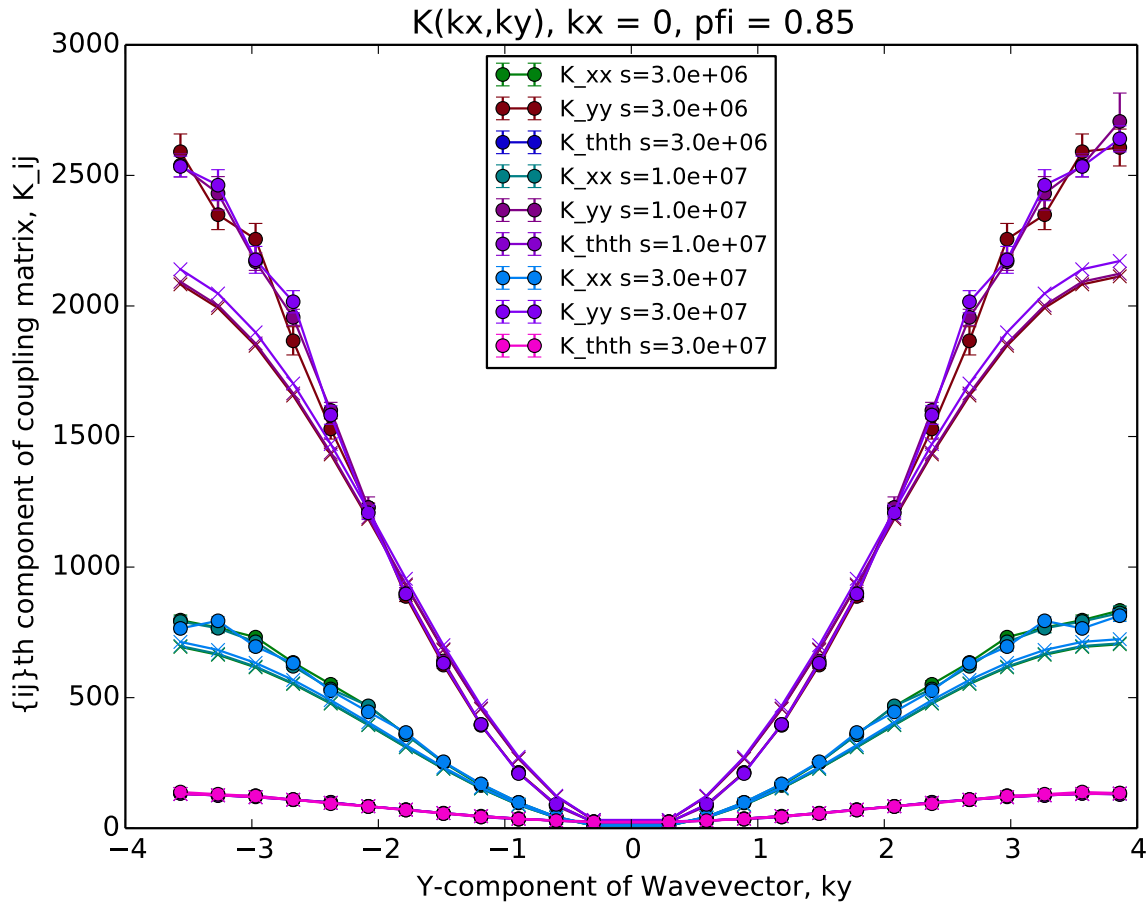
Figure 2: $N = 676$ and $\phi = 0.850$. For a sufficiently dense crystal, running the simulation longer than 3×10^6 sweeps doesn't change the dispersion curves at all.
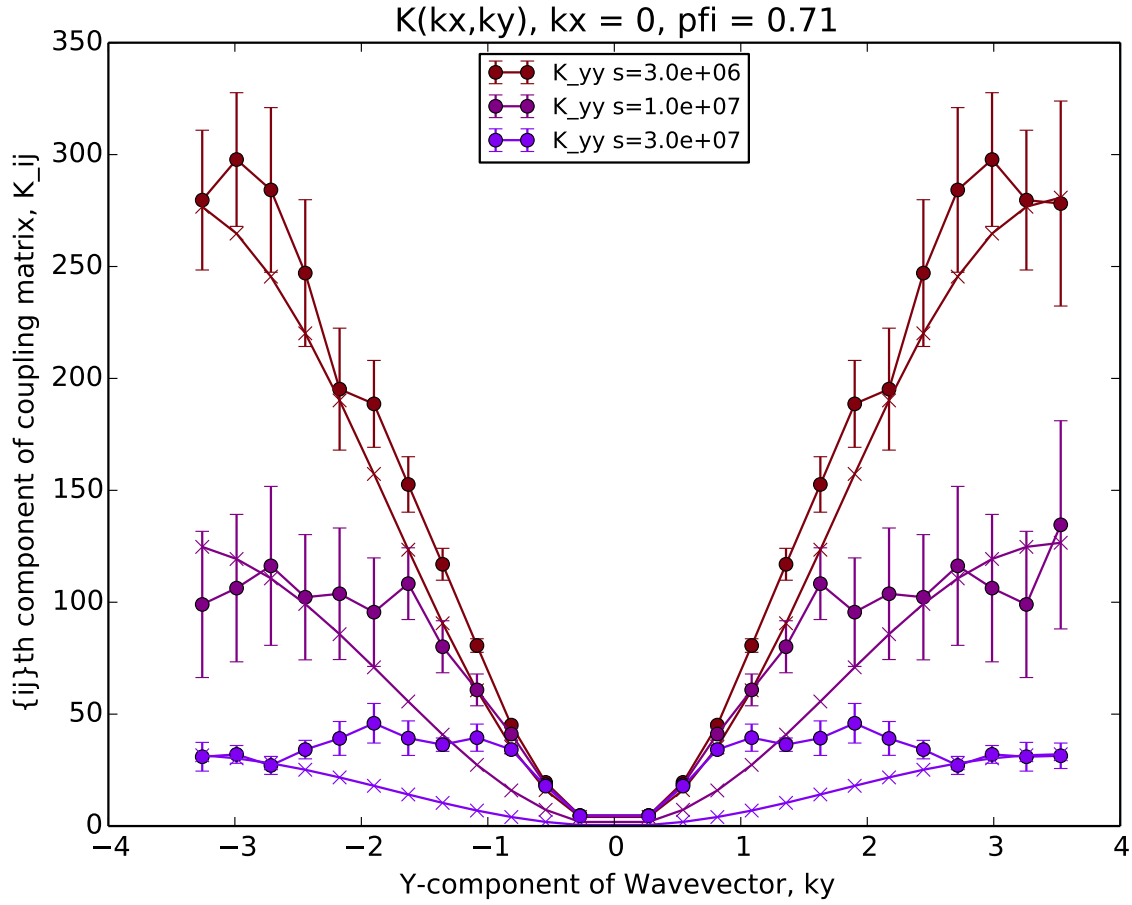
Figure 3: $N = 676$ and $\phi = 0.710$. Only the longitudinal phonon is shown for clarity. The dispersion curve changes drastically as the simulation runtime is increased. Error bars are significantly reduced, and had the simulation not been run for longer, I would have mistakenly assumed that the phonon mode had survived even down to $\phi = 0.710$. Clearly, though, long-time correlations play a large role.
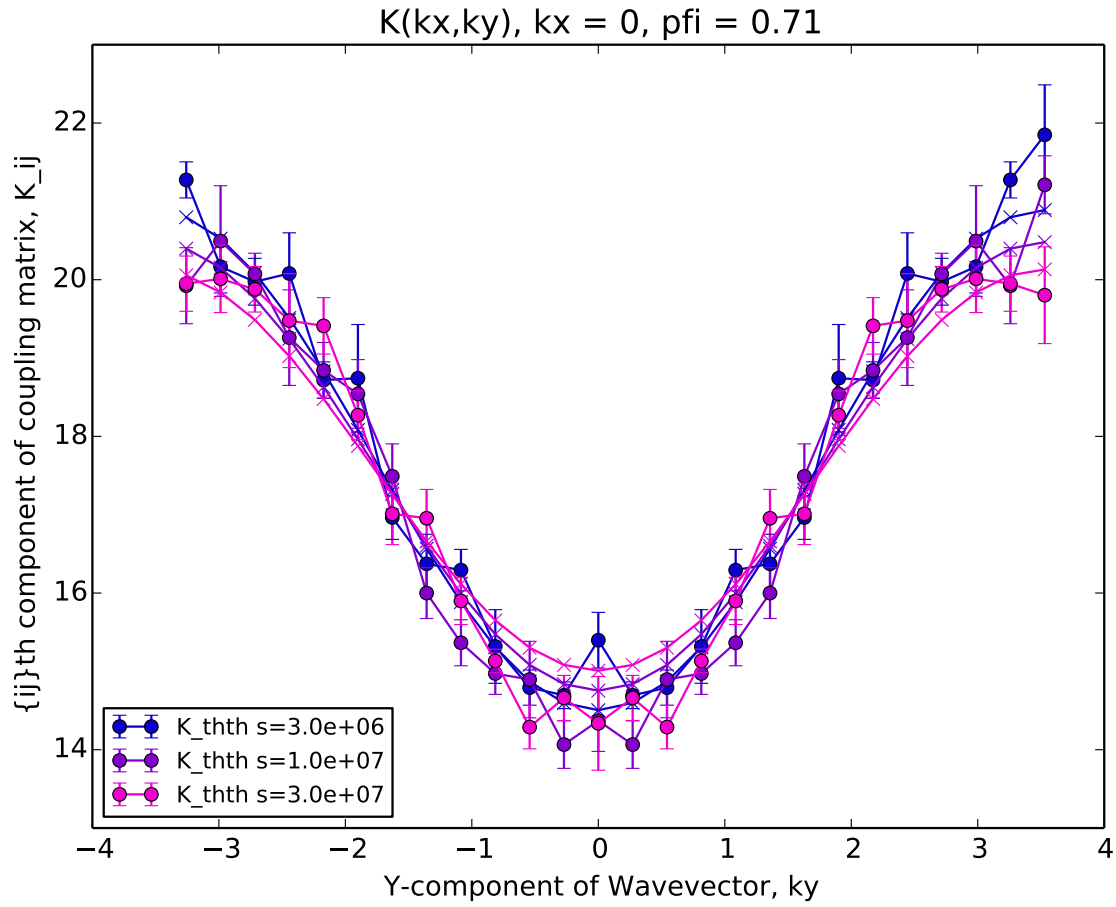
Figure 4: $N = 676$ and $\phi = 0.710$, same conditions as Figure 3. Though the phonon mode was very sensitive to the time sampling, the libron mode shows robustness, because this mode survives the crystal melting transition into the hexatic phase.
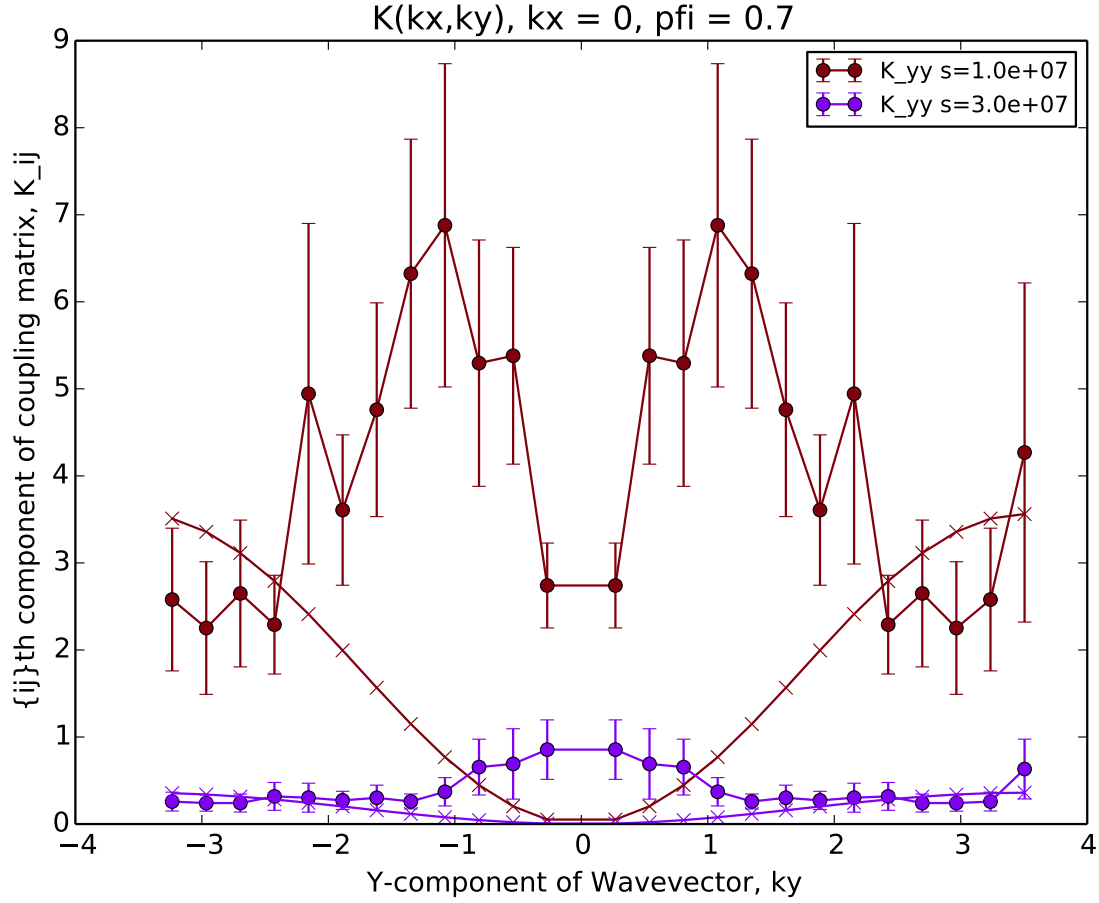
Figure 5: $N = 676$ and $\phi = 0.700$. The phonon mode is totally extinguished at this density, as shown by the longer-time simulation. There are large error bars associated with long-wavelength modes, which is not surprising because dislocation defects pervade the system at this density, so phonons on short length scaled (large k-vectors) will be well resolved, but small k-vector phonons will not. The $s = 3 \times 10^6$ simulation is not even shown because it is such garbage.
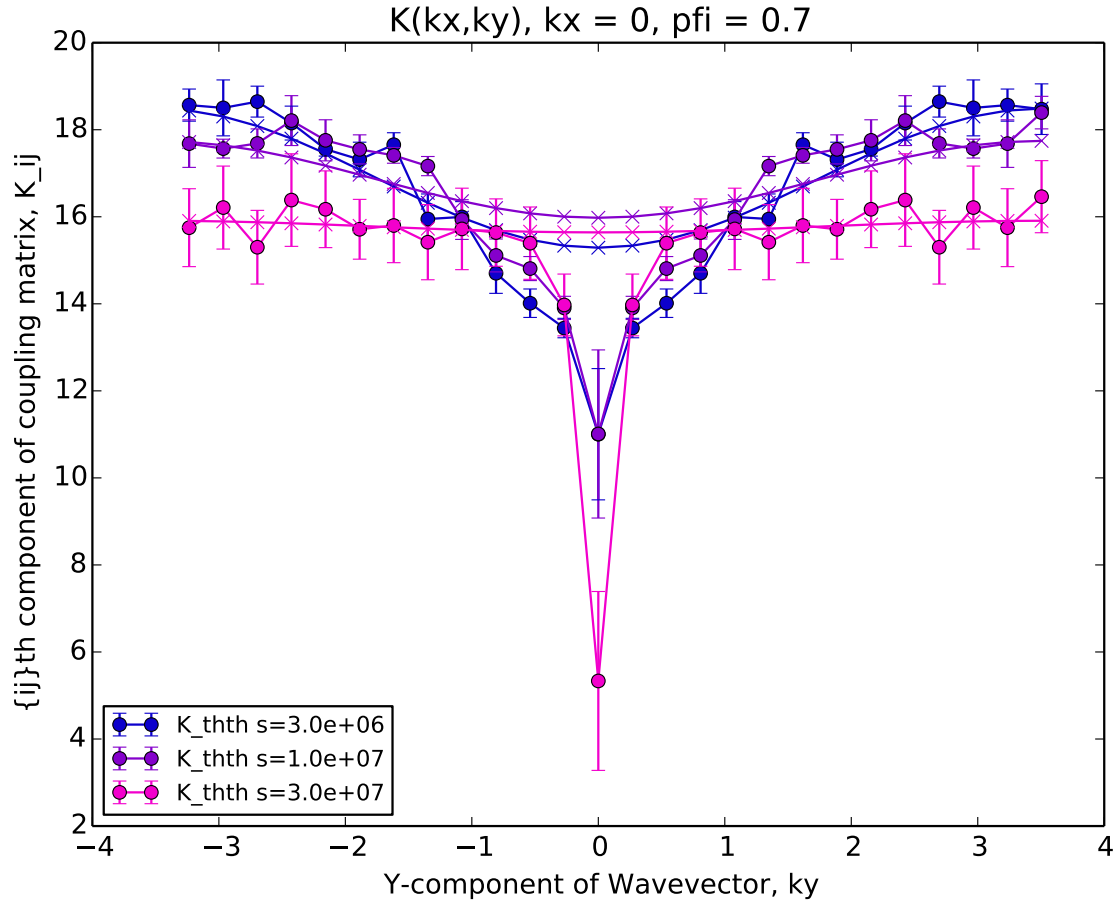
Figure 6: $N = 676$ and $\phi = 0.700$. The libron mode is beginning to show large deviations as a function of simulation time at this density. We're nearing the hexatic phase transition density, which is somewhere around 0.69

The main takeaway of Figures 2–6 is that either longer simulations need to be run or the sampling period needs to be changed as the critical point is approached. The latter is clearly the simplest method, but it reduces the number of independent frames to create correlation functions from.

4   Finite size effects

All the following figures are for $N = 26^2, 50^2$ and 100^2 at $s = 10^7$. They show densities $\phi = 0.800, 0.710$ and 0.700.
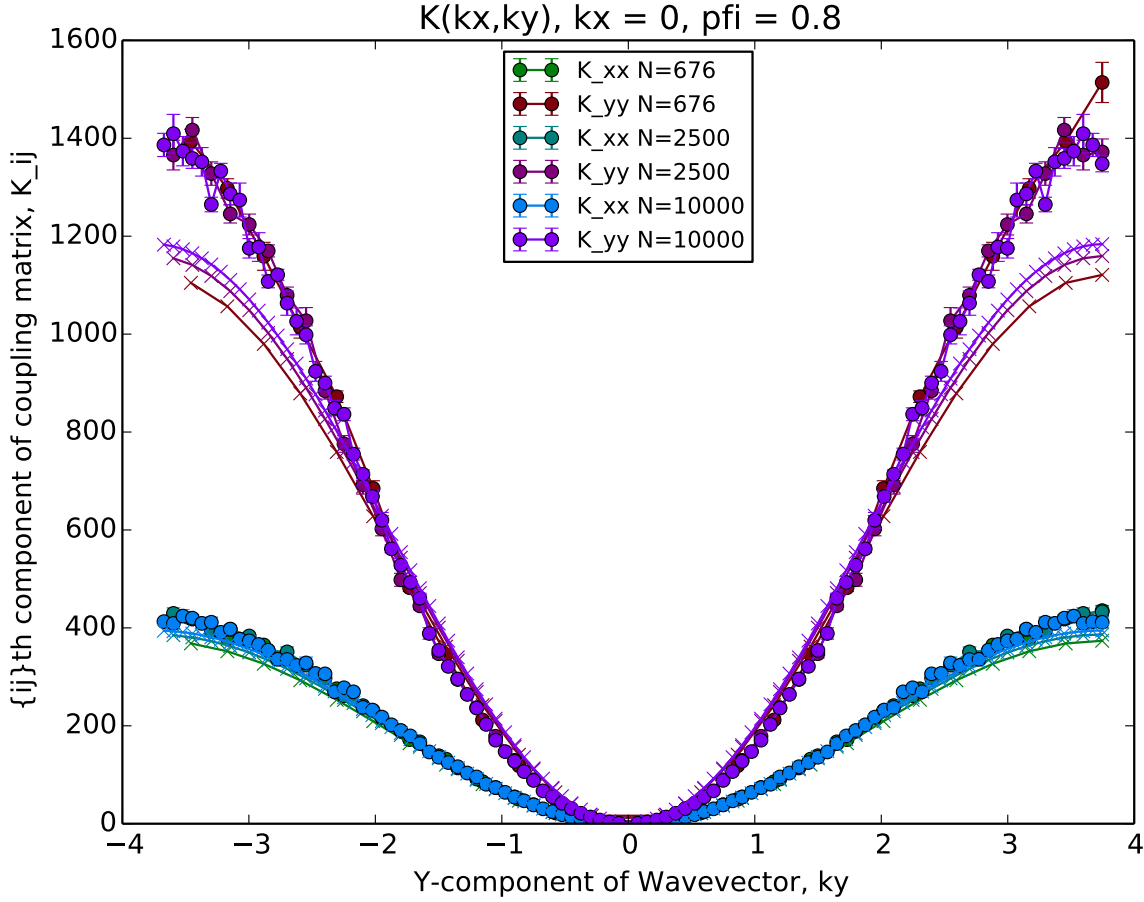
Figure 7: Phonon dispersion for three systems at $\phi = 0.8$. The simulation data are essentially identical, and the theoretical curves vary by about 2%. The $N = 100^2$ curve has the advantage of having finer resolution in k-space, but the $N = 26^2$ curve takes far less time to run. The theoretical curves show striking systematic error for large values of k_y, and I don't quite understand why. This suggests that, at this density, more is going on at short length scales than just nearest neighbor interactions.
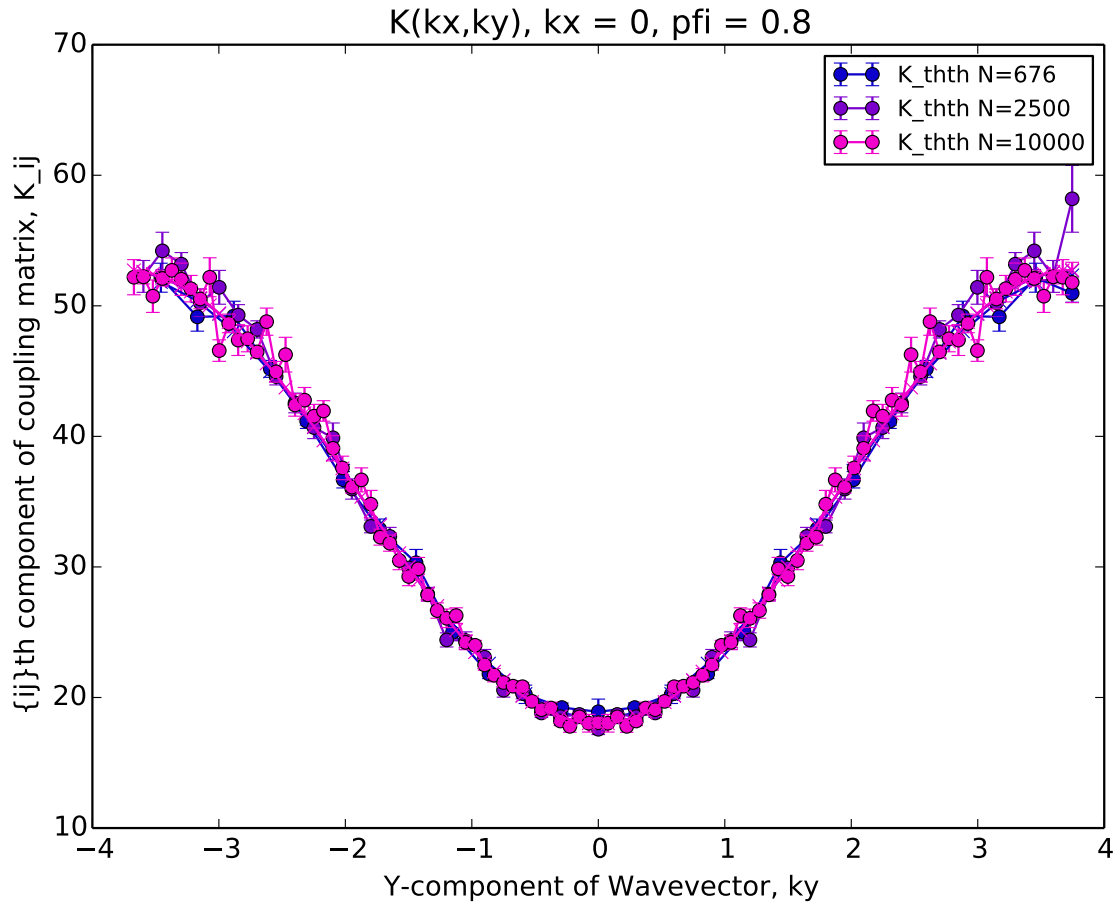
Figure 8: Libron dispersion of the same system as Figure 7. There is no sacrifice made at all by running small simulations to explore the libron dynamics at high densities.
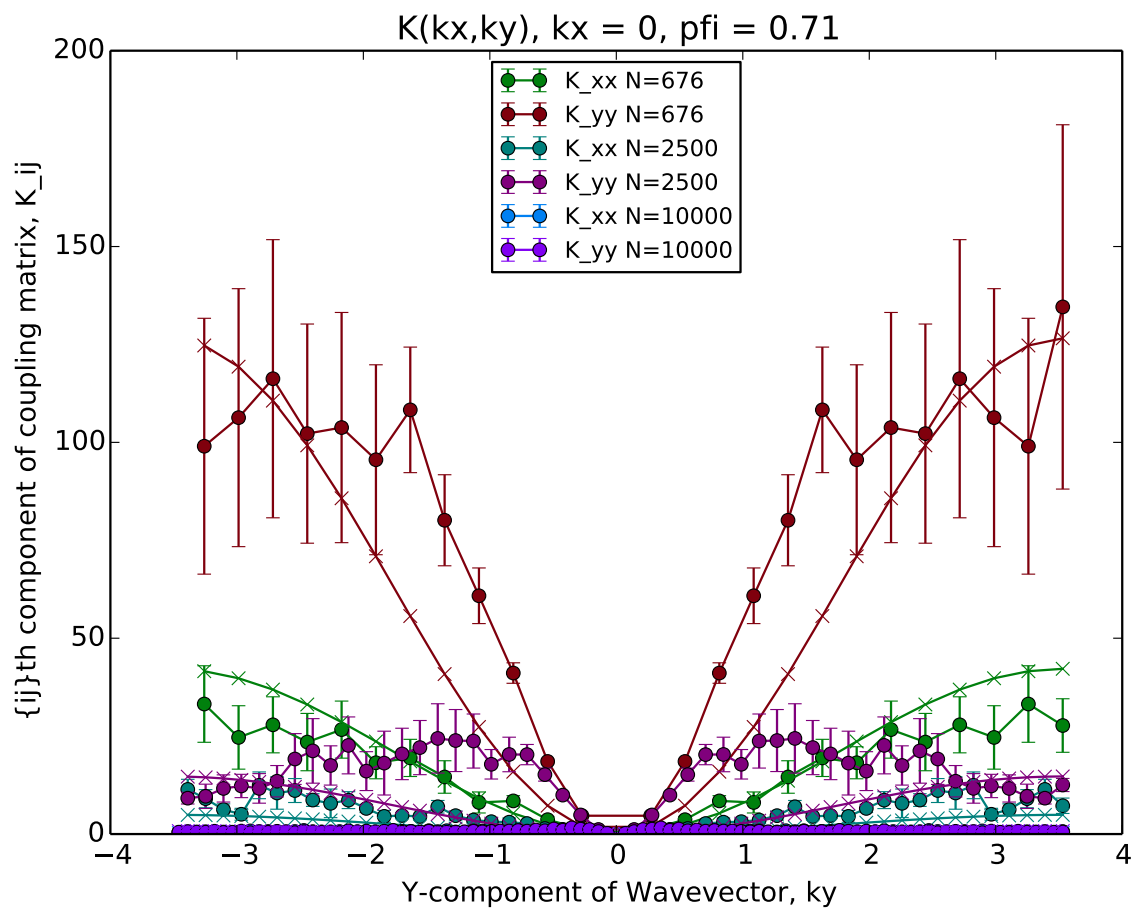
Figure 9: Phonon modes at density of $\phi = 0.710$. The small systems show unacceptable error in that it predicts the phonon has significant dispersion at this density. Figure 10 shows the bottom of the graph in more detail.
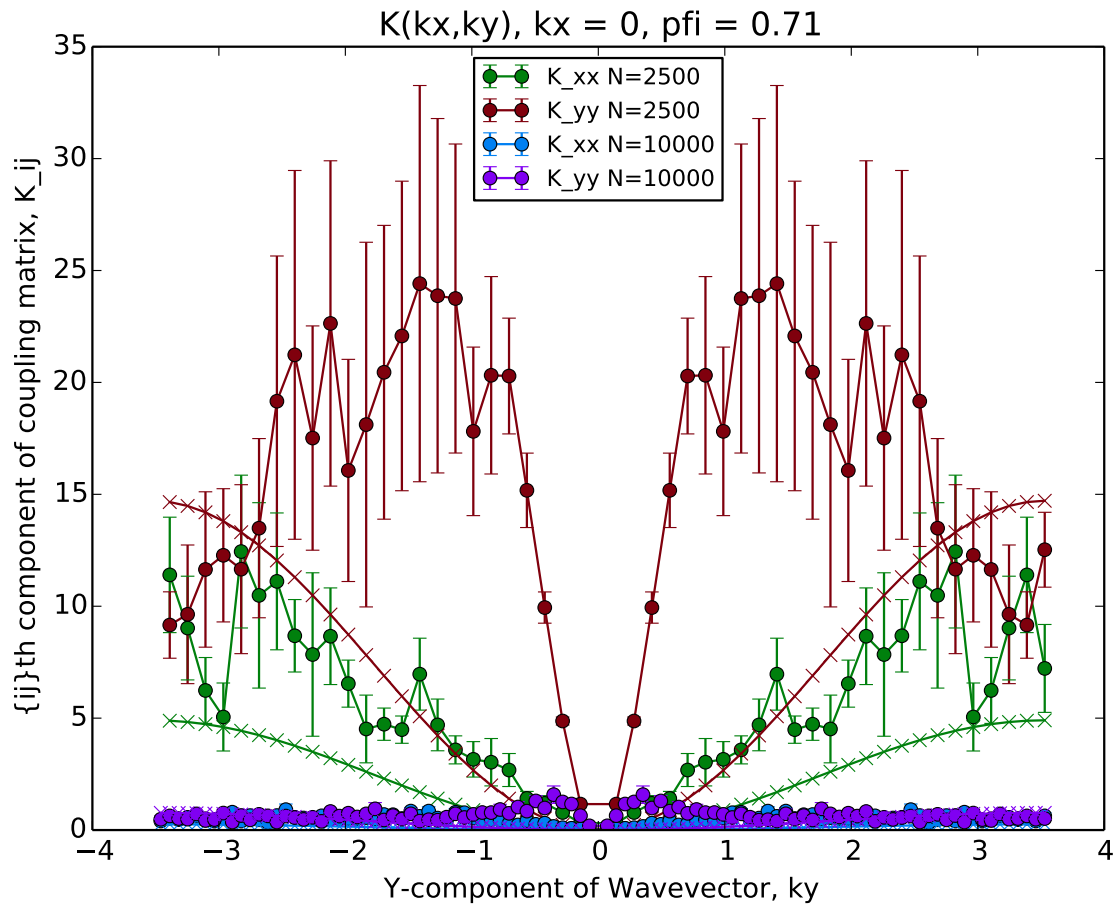
Figure 10: Phonon modes in same system as Figure 9. Compared to the $N = 100^2$ simulations, the $N = 50^2$ simulations are unacceptable as well.
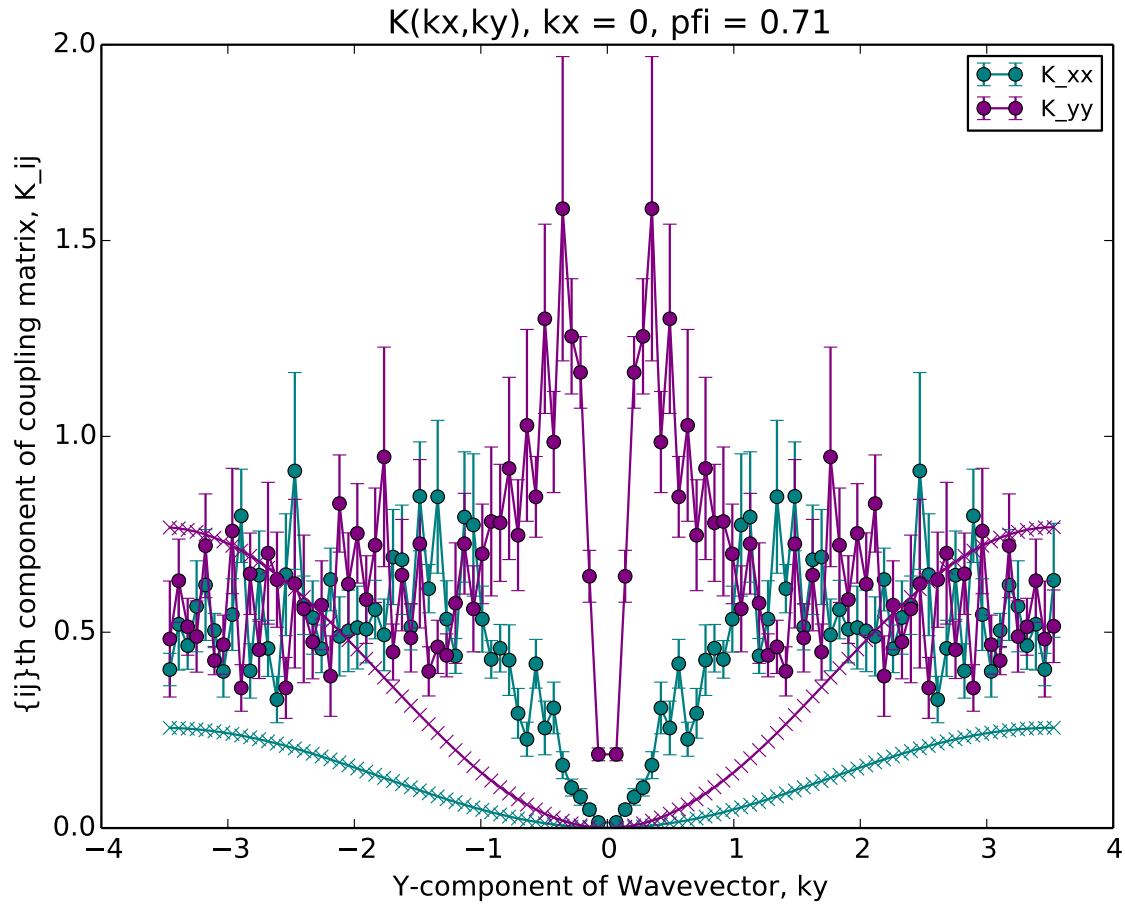
Figure 11: Phonon modes in same system as Figure 9 only at $N = 100^2$. The phonon dispersion is very flat and has large fluctuations at low wavelength, which is to be expected of any finite-sized system. This is really as good as it's going to get without running enormous simulations.
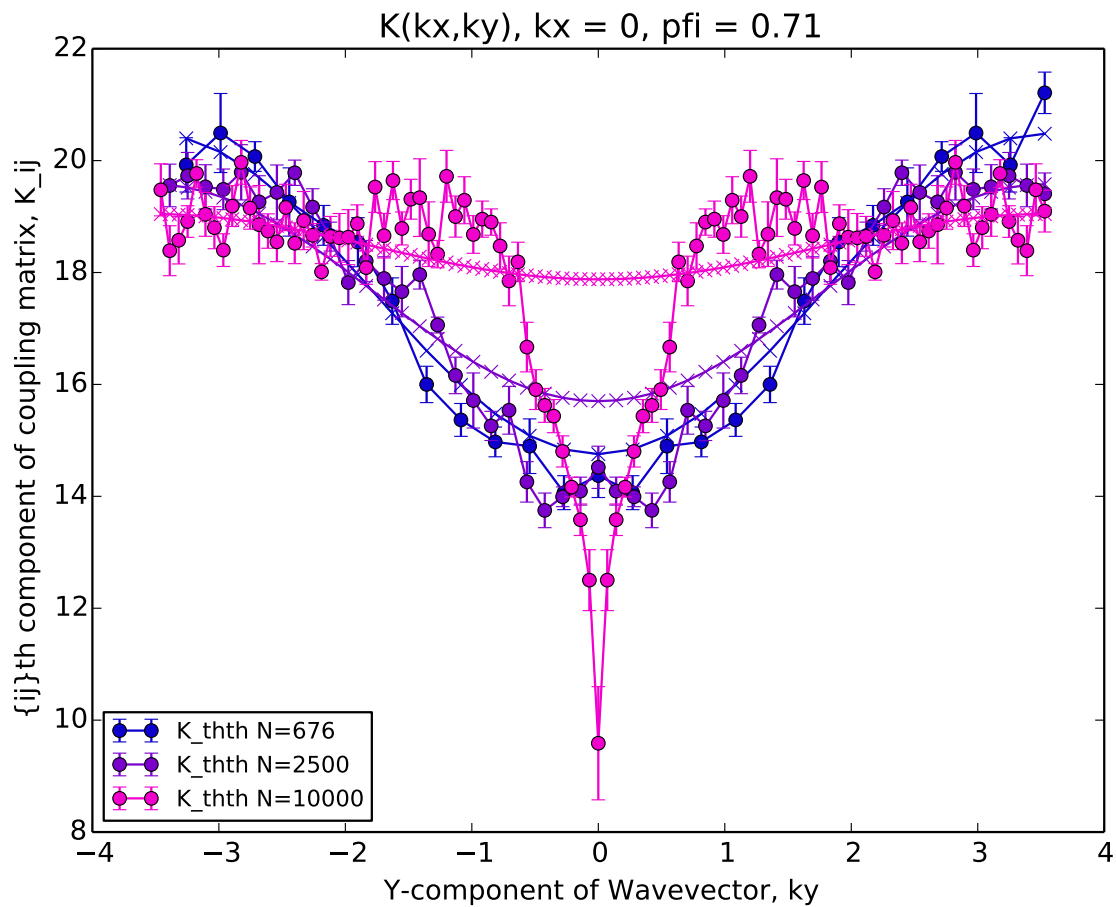
Figure 12: Libron mode in same system as Figure 9. The modes of characteristically small length scales (large k-vectors) are unaffected by increasing system size, but going to large systems elucidate long-wavelength dynamics.
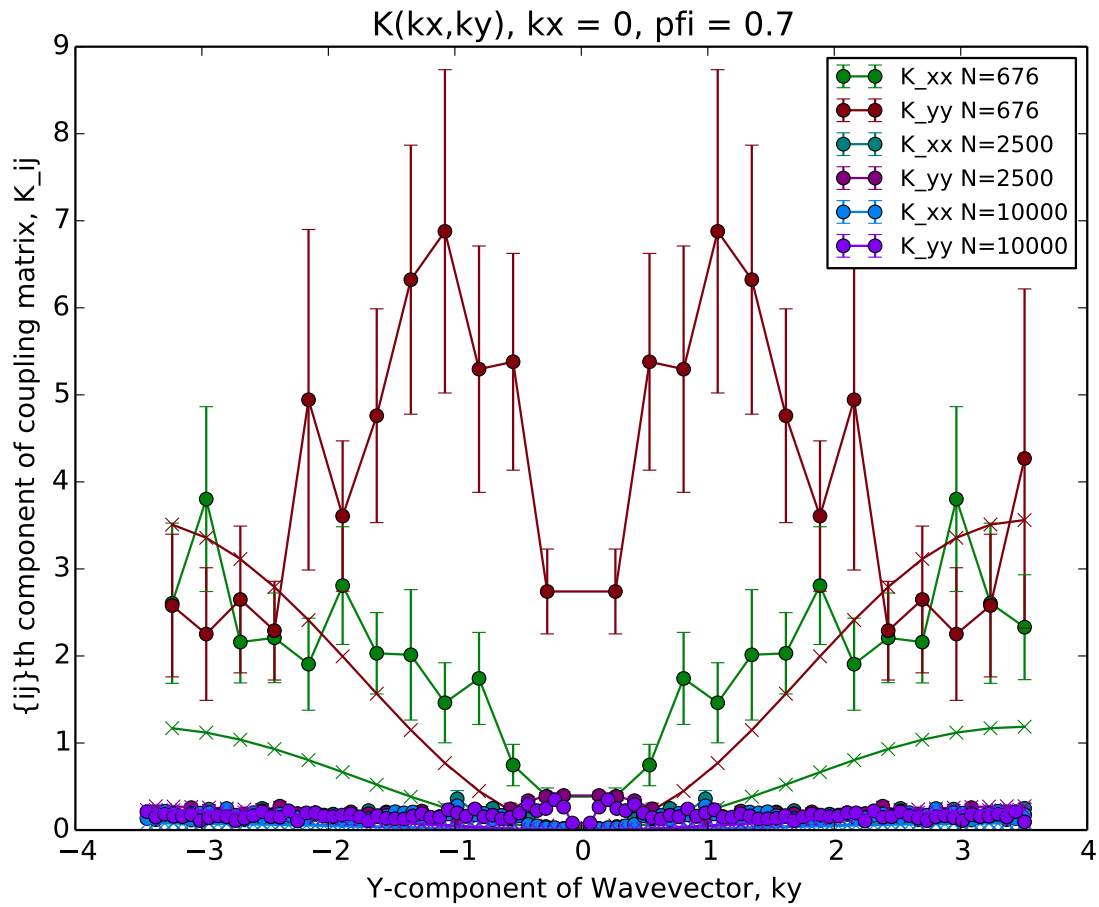
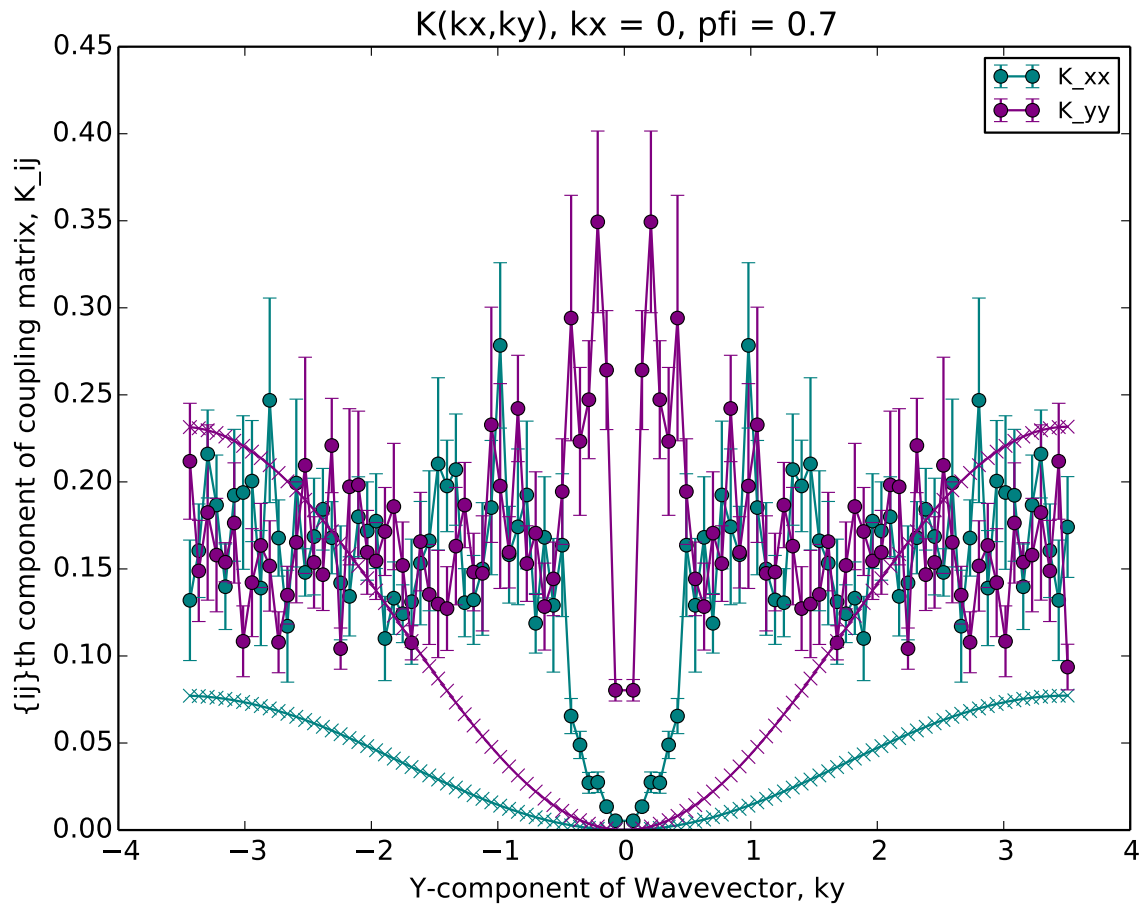Figure 13: Phonon modes at density of $\phi = 0.700$. The small systems are essentially hot garbage.

Figure 14: Phonon modes at density of $\phi = 0.700$ and system size of just 100^2. Not totally garbage but it tells us that the phonon is essentially gone at this density.
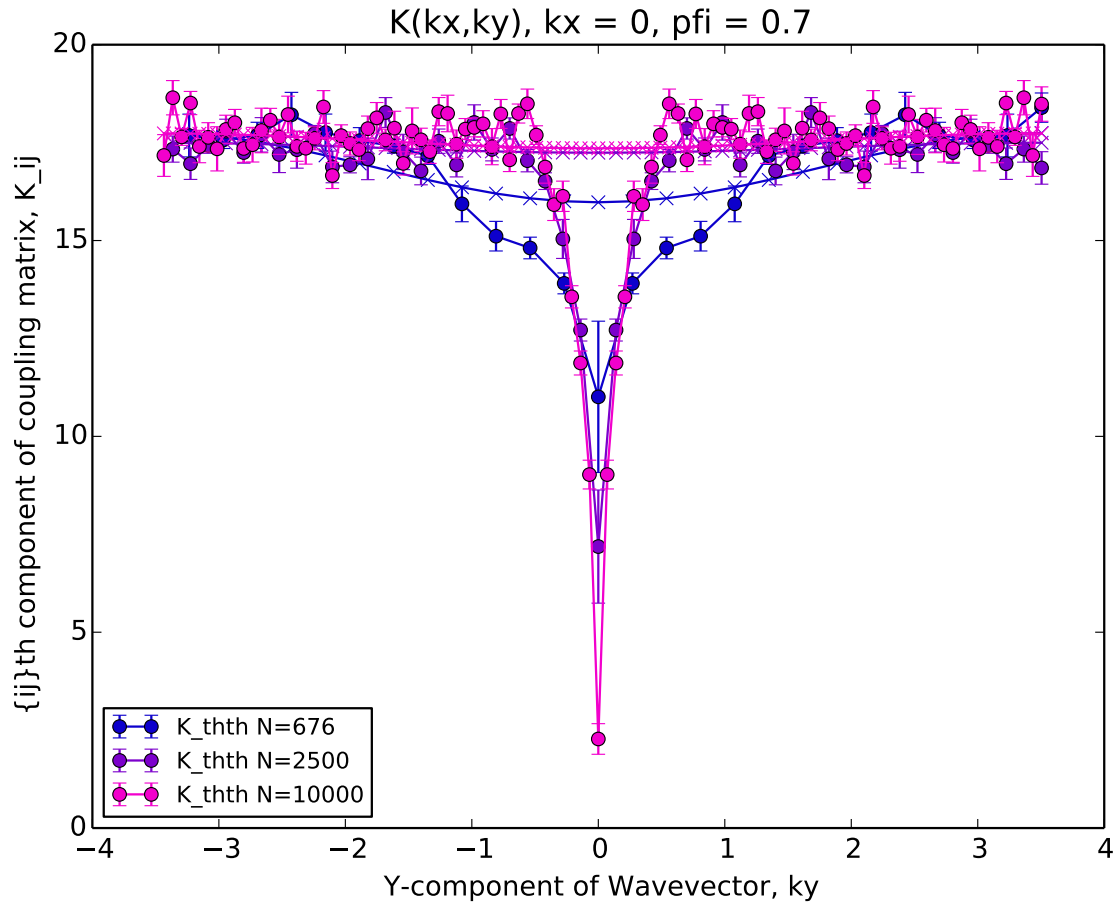
Figure 15: Libron modes at density of $\phi = 0.700$. Most of them agree that the libron dispersion is going flat but the larger simulations tell us that its $\mathbf{k} = 0$ mode frequency is also approaching zero.

The takeaway from this comparison of finite size effects is that the $\mathbf{k} = 0$ mode is sensitive to the number of particles in the system and the distance from the critical point. Small simulations are deceptive
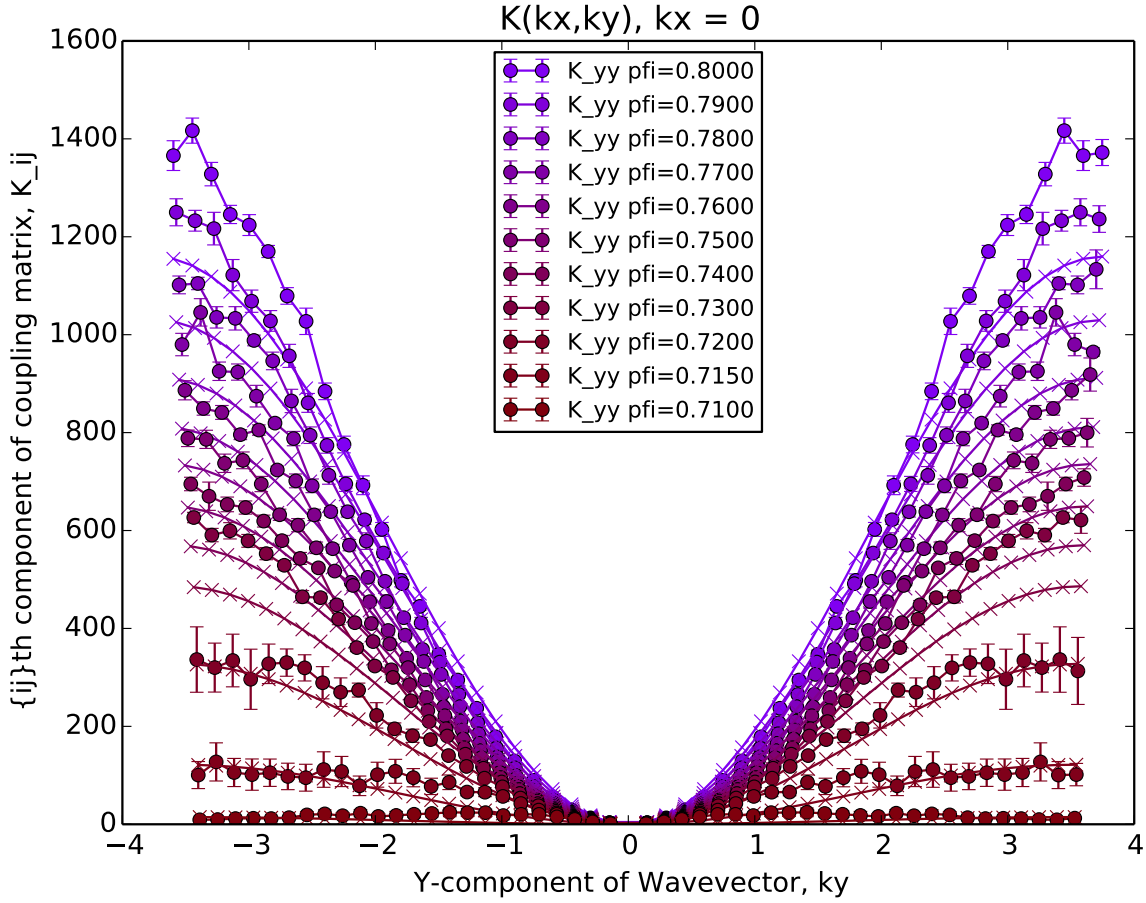
5   Packing fraction effects

Figure 16: Longitudinal phonon for $N = 50^2$ and $s = 10^7$ and for ϕ decreasing from 0.800 to 0.710. The first major jump occurs between 0.730 and 0.720, then another one from 0.720 to 0.715. Note also that the theoretical curves fail to fit the phonon dispersion for large $|\mathbf{k}|$ at higher densities.
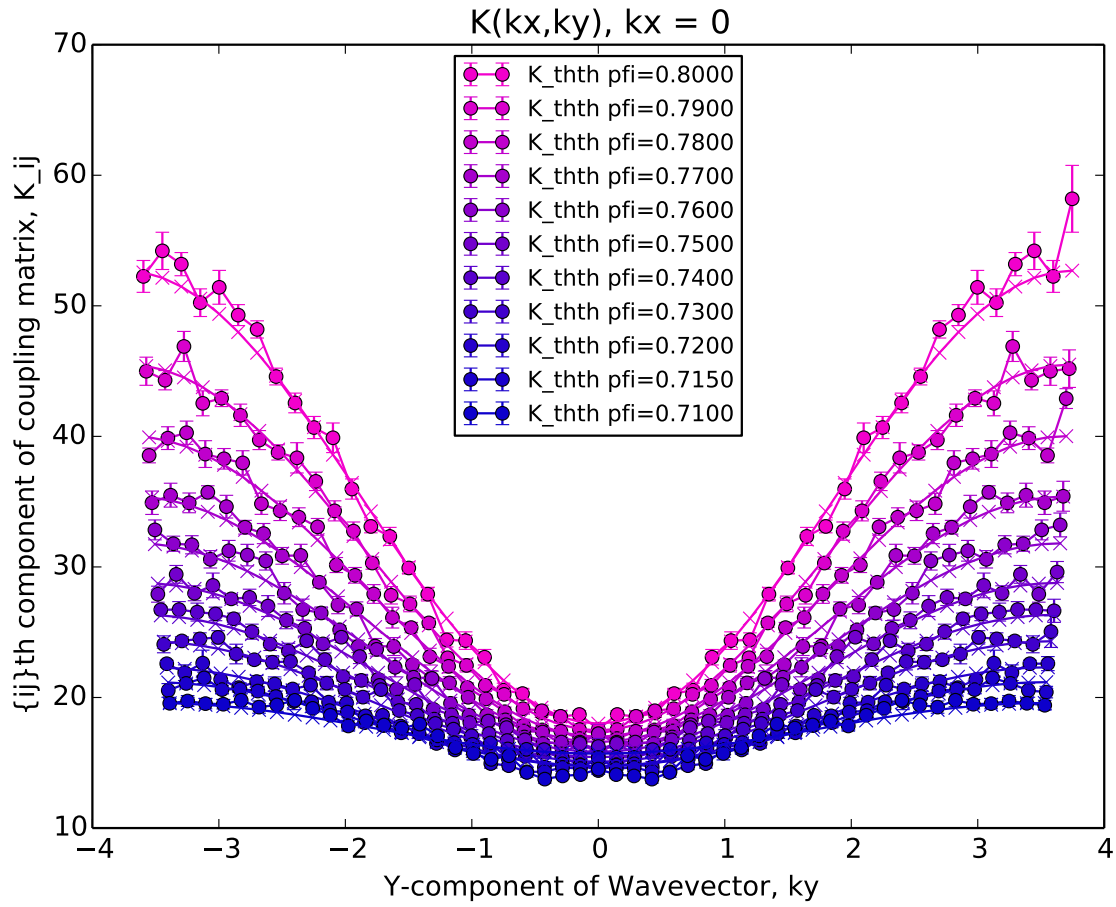
Figure 17: Libron for $N = 50^2$ and $s = 10^7$ and for ϕ decreasing from 0.800 to 0.710. The libron dispersion is more or less smooth as the density is decreased, unlike the phonon dispersion.
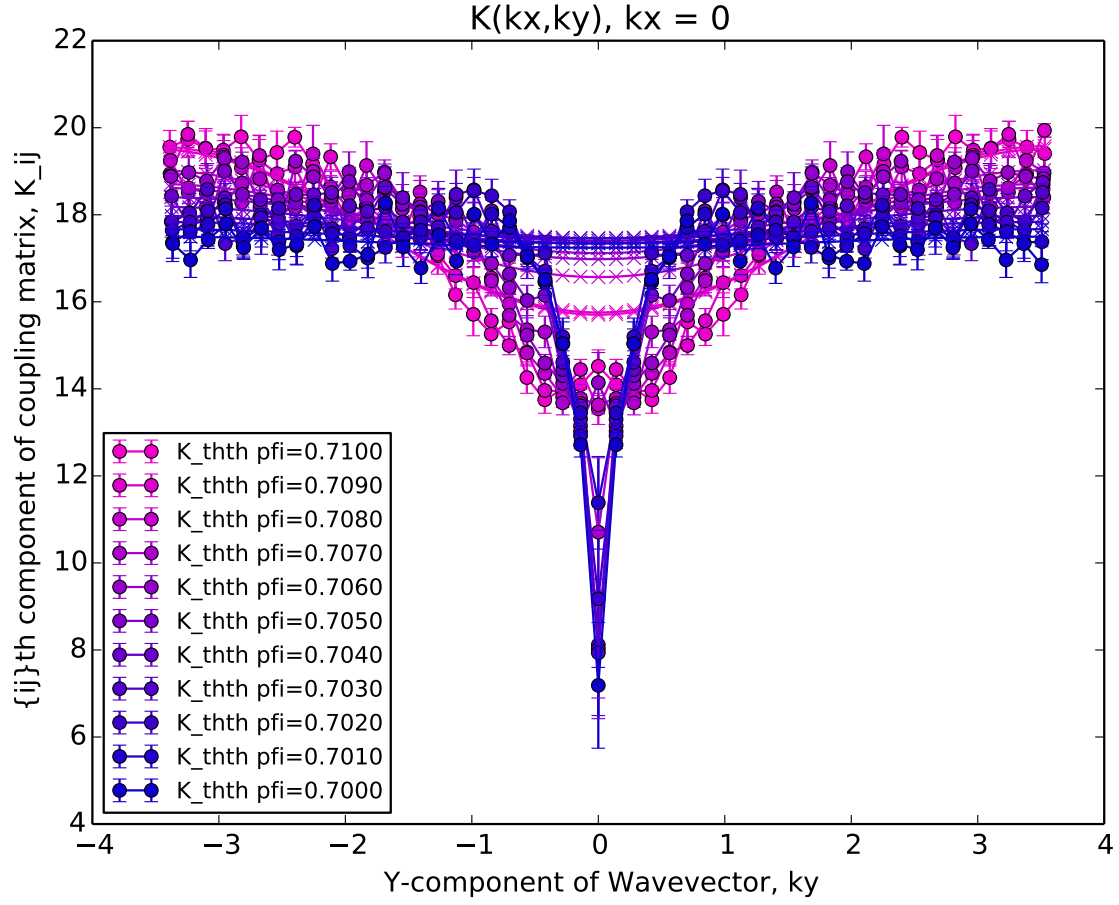
Figure 18: Libron for $N = 50^2$ and $s = 10^7$ and for ϕ decreasing from 0.710 to 0.700. The libron dispersion deviates more and more from predicted theory curves as the density is decreased. Large k dispersion is relatively flat near $\phi = 0.700$ and the $\mathbf{k} = 0$ mode frequency decreases with decreasing density.
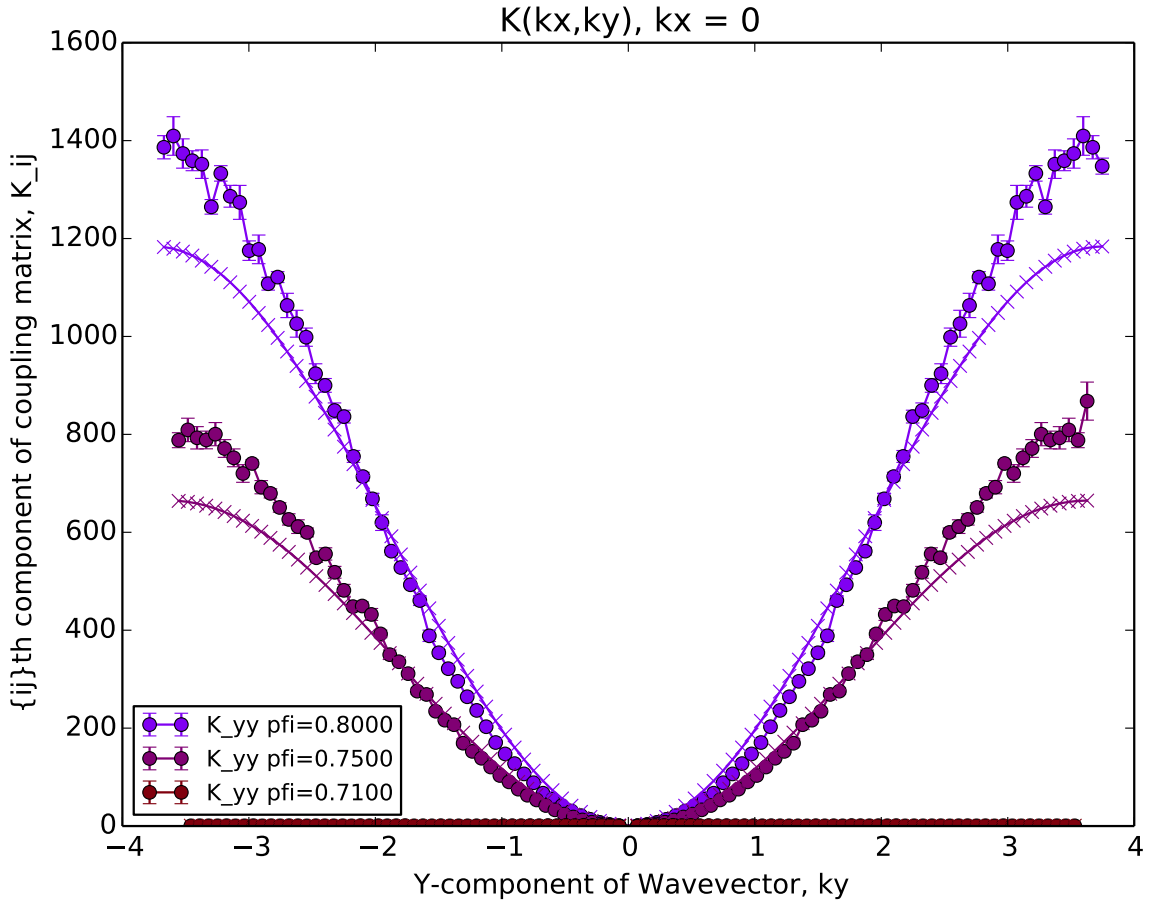
Figure 19: Longitudinal phonon for $N = 100^2$ and $s = 10^7$ and for ϕ decreasing from 0.800 to 0.710. These simulations were very long, so the resolution of Figure 16 would have been wasteful. The same features are present, a jump to a near flat dispersion around $\phi = 0.710$. Figure 20 shows lower ϕ with a smaller y-axis.
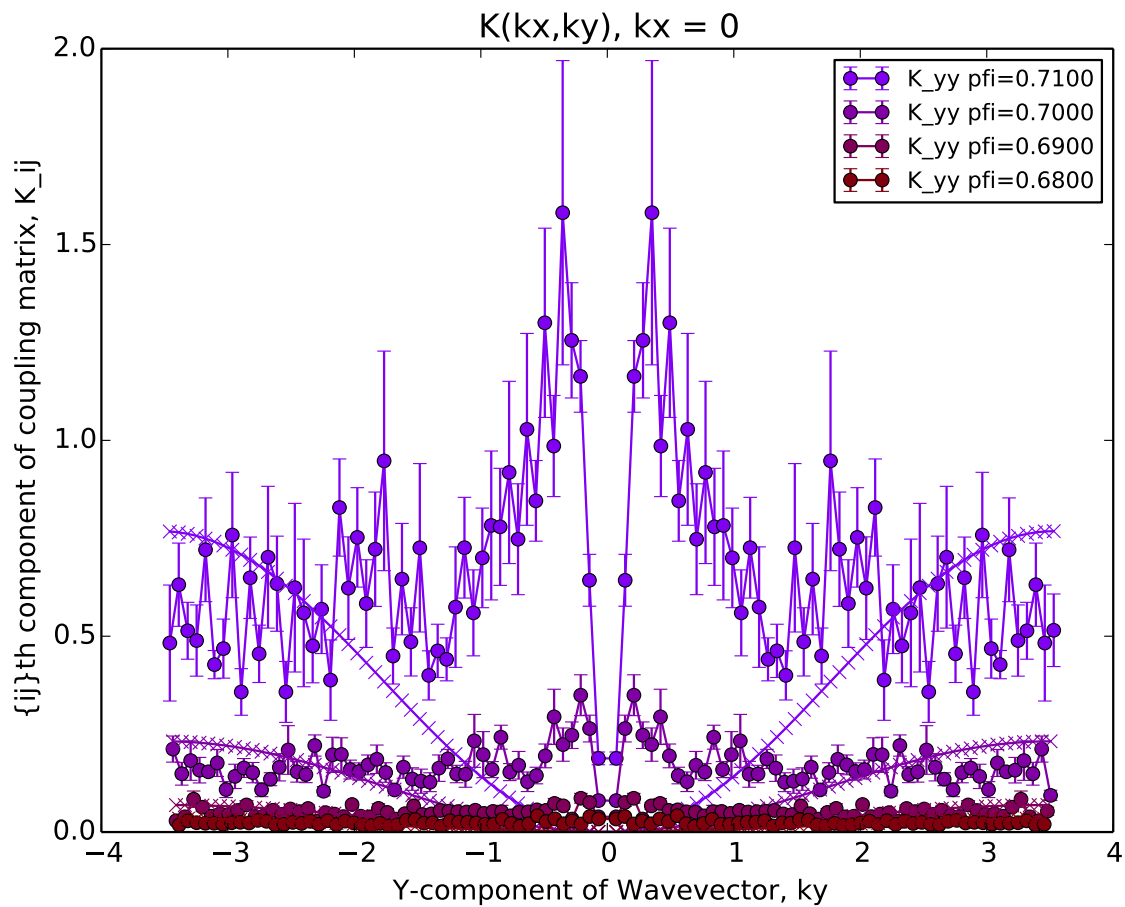
Figure 20: Longitudinal phonon for $N = 100^2$ and $s = 10^7$ and for ϕ decreasing from 0.710 to 0.680. Zooming in reveals that the dispersion curves don't fit the theory at all near the phase transition (to be expected), and error bars are very large compared to the magnitude of the dispersion itself.
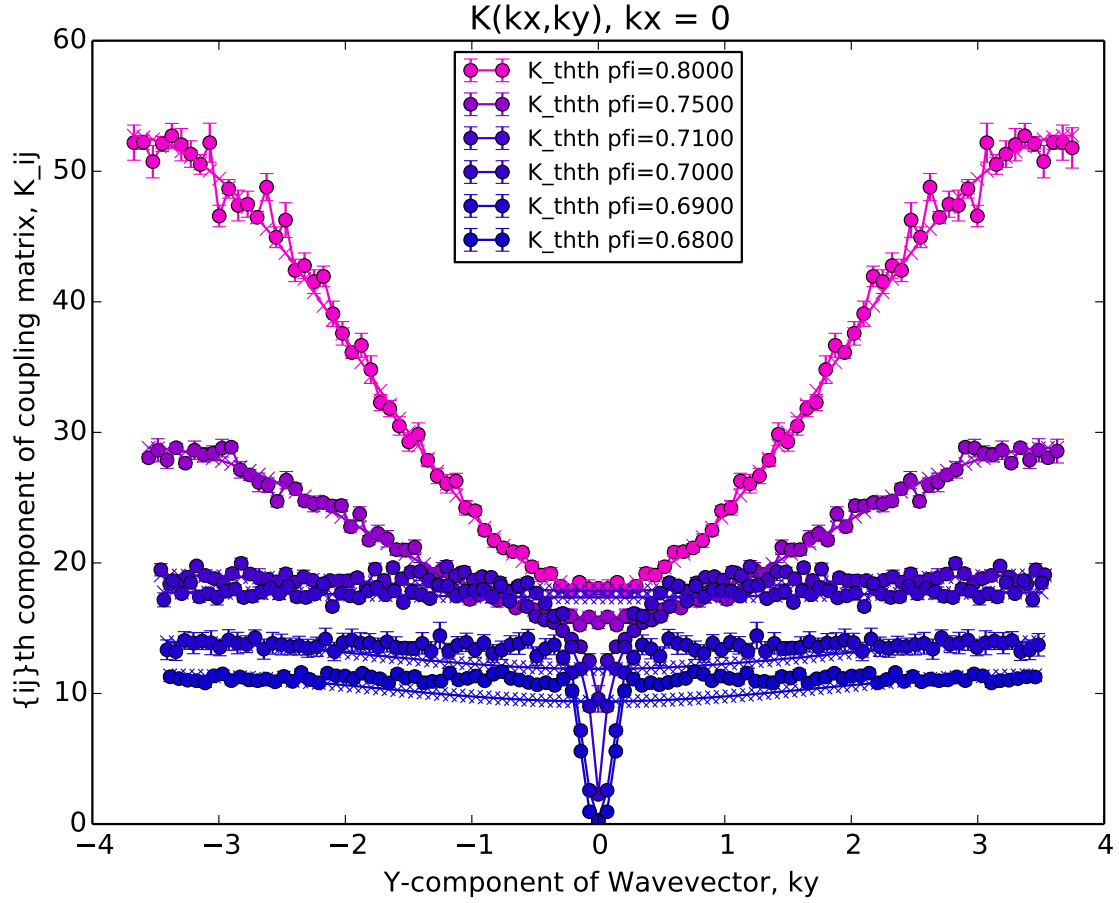
Figure 21: Libron dispersion for $N = 100^2$ and $s = 10^7$ and for ϕ decreasing from 0.800 to 0.680. As the density is lowered through the crystal→hexatic transition and closer to the hexatic→ fluid transition, the libron's dispersion becomes flatter for $k > 0$ and the $\mathbf{k} = 0$ mode continues to move towards 0. Once $\omega(\mathbf{k} = 0) = 0$, this signifies a density at which the libron mode is no longer massive and a uniform rotation of the hexagons no longer costs energy (or rather entropy). The lower densities are provided in zoom in Figure 22
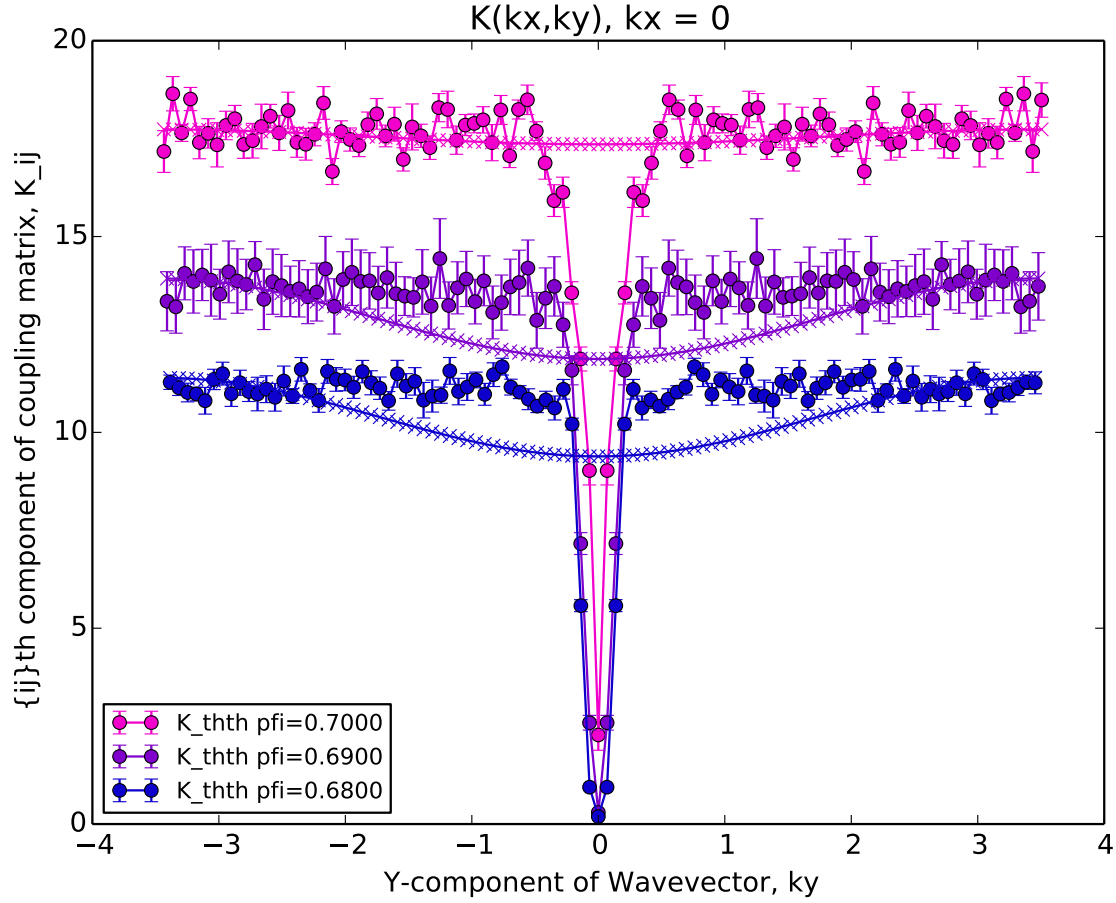
Figure 22: Same as Figure 21 but only for lower densities. It may not be clear, but the error bars near $k = 0$ are actually very small, compared to the error bars at $k > 0$.

Near phase transitions, the phonon and libron spectra can become flat. I'd like to explore and explain what that signifies. The potential energy part of the Hamiltonian expressed in terms of the Fourier components of the libron field $\tilde{\theta}_{\mathbf{k}}$ (I'll just use the libron field for simplicity, and without loss of generality, because the librons and phonons are uncoupled at these densities anyway) is

$$\mathcal{H} = \frac{1}{2} \sum_{\mathbf{k}} \tilde{\theta}_{\mathbf{k}}^* K_{\theta\theta,\mathbf{k}} \tilde{\theta}_{\mathbf{k}}. \tag{6}$$

Now, if we consider that the matrix $K_{\theta\theta,\mathbf{k}}$ is *totally independent* of the wavevector $\mathbf{k}$, which is the case if the dispersion curve is *totally flat*, then we can pull it out of the sum and perform the inverse Fourier transform:

$$\mathcal{H} = \frac{1}{2} K_{\theta\theta} \sum_{\mathbf{k}} \tilde{\theta}_{\mathbf{k}}^* \tilde{\theta}_{\mathbf{k}} = \frac{1}{2N} K_{\theta\theta} \sum_{\mathbf{k}} \sum_{\mathbf{r}_i} \sum_{\mathbf{r}_j} \theta_i \theta_j e^{i\mathbf{k} \cdot (\mathbf{r}_i - \mathbf{r}_j)}. \tag{7}$$

The orthogonality of the exponentials means that $\sum_{\mathbf{k}} e^{i\mathbf{k}\cdot(\mathbf{r}_i - \mathbf{r}_j)} = N\delta_{ij}$, which then gives us back the real space Hamiltonian:

$$\mathcal{H} = \frac{1}{2} K_{\theta\theta} \sum_i \theta_i^2. \tag{8}$$

This is a set of uncoupled harmonic oscillators with spring constant $K_{\theta\theta}$, and if we use the generalized equipartition theorem (Eq. 2), we see that

$$\langle \theta_i \theta_j \rangle = \frac{k_B T}{K_{\theta\theta}} \delta_{ij}. \tag{9}$$

No orientational degree of freedom is correlated with any other degree of freedom. Yet, they still appear in the Hamiltonian and cost energy, evidently. This isn't exactly the right way to think about it. The fact that $K_{\theta\theta,\mathbf{k}=0} \to 0$ should be important. If we let $K_{\theta\theta,\mathbf{k}=0} = 0$ strictly, then we'll have an uninvertible matrix, so let's let it go to $\epsilon K_{\theta\theta}$ to see what happens. So let's put that in:

$$\mathcal{H} = \frac{1}{2} K_{\theta\theta} \sum_{\mathbf{k}\neq 0} \tilde{\theta}_{\mathbf{k}}^* \tilde{\theta}_{\mathbf{k}} + \frac{1}{2} K_{\theta\theta} \epsilon = \frac{1}{2} K_{\theta\theta} \sum_{\mathbf{k}} \tilde{\theta}_{\mathbf{k}}^* \tilde{\theta}_{\mathbf{k}} - \frac{1}{2} K_{\theta\theta}(1-\epsilon)\tilde{\theta}_0^* \tilde{\theta}_0. \tag{10}$$

Performing the inverse Fourier transform:

$$\mathcal{H} = \frac{1}{2} K_{\theta\theta} \sum_i \theta_i^2 - \frac{1}{2N} K_{\theta\theta}(1-\epsilon) \sum_{i,j} \theta_i \theta_j. \tag{11}$$

$$\mathcal{H} = \frac{1}{2N} K_{\theta\theta} \boldsymbol{\theta} \cdot \begin{pmatrix} N-1+\epsilon & -1+\epsilon & -1+\epsilon & -1+\epsilon & \cdots \\ -1+\epsilon & N-1+\epsilon & -1+\epsilon & -1+\epsilon & -1+\epsilon \\ -1+\epsilon & -1+\epsilon & N-1+\epsilon & -1+\epsilon & -1+\epsilon \\ -1+\epsilon & -1+\epsilon & -1+\epsilon & N-1+\epsilon & -1+\epsilon \\ \vdots & -1+\epsilon & -1+\epsilon & -1+\epsilon & \ddots \end{pmatrix} \cdot \boldsymbol{\theta} = \frac{1}{2} \theta_i K_{ij}' \theta_j \tag{12}$$

Mathematica gives us the unintuitive result that the inverse of this matrix (which is proportional to the correlation function matrix of all the orientational degrees of freedom) is

$$K_{ij}'^{-1} = \frac{1}{\epsilon N K_{\theta\theta}} \begin{pmatrix} 1+(N-1)\epsilon & 1-\epsilon & 1-\epsilon & \cdots \\ 1-\epsilon & 1+(N-1)\epsilon & 1-\epsilon & 1-\epsilon \\ 1-\epsilon & 1-\epsilon & 1+(N-1)\epsilon & 1-\epsilon \\ \vdots & 1-\epsilon & 1-\epsilon & \ddots \end{pmatrix}. \tag{13}$$

At this point I'd like to pause to interpret these results. The determinant of the matrix $\mathbf{K}'(\epsilon)$ is $\mathcal{O}(\epsilon)$. What this tells us is that if we let $\epsilon \to 0$ exactly, $\mathbf{K}'$ will no longer have an inverse and correlation functions will no longer be finite. The $\mathbf{k} = 0$ mode is *floppy*. However, if we examine the components of K_{ij}', all the off-diagonal components are nonzero and of order $1/N$, whereas the diagonal components are of order 1. There is *nonzero coupling to every particle in the system* but there is *no cost to rotating all the particles the same amount*. That is, we can send every $\theta_i \to \theta_i + \Delta\theta$ and it wouldn't cost any energy. However, *every particle is weakly coupled to every other particle*, and by weakly, it is meant that the coupling between θ_i and θ_j is order $1/N$ (but there are $\sim N$ degrees of freedom that θ_i is coupled to, so it is weakly coupled to the whole system by $\mathcal{O}(1)$ interactions). The way I am interpreting this is that this represents an ideal gas that is coupled in a mean-field manner to itself, just like the infinite-range Ising model.

6   Next-nearest-neighbor and nonlinear effects

7   Topological properties of defects